STAG: Smart Tools and Applications in Graphics (2018)
M. Livesu, G. Pintore and A. Signoroni (Editors)

Adaptive environmental sampling: The interplay between geostatistics and geometry

S. Berretta[1] and D. Cabiddu[1] and S. Pittaluga[1] and M. Mortara[1] and M. Spagnuolo[1] and M. Vetuschi Zuccolini[2]

[1]IMATI CNR, Genova, Italy
[2]DISTAV University of Genova, Italy

Abstract

In environmental surveys a large sampling effort is required to produce accurate geostatistical maps representing the distribution of environmental variables, and the analysis of each sample is often expensive. Typically, the sample locations are completely specified in the survey design phase, prior to data-collection. Usually, the sampling points are located on a regular grid, or along directions that are selected with respect to any a-priori knowledge of the expert. No feedback is available during the survey.
In this paper, we present a different sampling strategy, namely adaptive sampling. *Our approach exploits geostatistics constructs in order to determine on-the fly the next best sample location. After initializing the system with few sampling points, an iterative routine predicts the variable distribution from the data sampled so far, and suggests the next sample to be acquired in order to optimize the uncertainty of the estimates. At every iteration a new sample is acquired, and the variable distribution map is refined, along with the uncertainty map related to that distribution. Our method allows to build a representation of the survey area as precise as the one provided by the traditional methods, but with less samples, thus reducing both time and costs of the survey. We show a preliminary evaluation of the adaptive strategy in the bi-dimensional case based on a synthetic scenario, and describe the generalization of these encouraging results to the full 3D domain in the concrete setting of water quality monitoring. A proper geometric representation of the three dimensional survey area, coupled with a proper visualization of distribution and related uncertainty, will provide real-time feedback during the survey.*

1. Introduction

Environmental monitoring includes the processes and activities needed to observe and characterize the trend of environmental variables. Environmental sampling is carried out, for instance, whenever there is a need to monitor contaminants in water, air or soil, and requires testing of hazardous sites, runoff into lakes, streams and seas, and air emissions from industry.

The standard way to plan an environmental survey provides several stages: first, all the locations where to collect physical samples are predetermined. In general, the sampling points are located on a regular grid, or along directions that are selected following a-priori knowledge. Then, the data collection takes place (no feedback is available during the survey); and finally, samples go under laboratory analysis. Afterwards, geostatistical maps are generated to represent the distribution of the examined environmental variables, and on the base of the results, additional surveys might be planned on subareas of the global domain, in order to refine the analysis only where the operator considers that it is needed. The operator is in charge of deciding where and how to refine the sampling, based on previous acquisitions and own knowledge. The campaign is therefore expensive, both in terms of money and time.

Furthermore, the monitoring is typically required in hazardous environments. In order to safeguard human operators, the use of robotic platforms (e.g., drones) to collect samples in dangerous areas is being investigated. Fortunately, the technological improvements now allow for direct measurements opposite to the sample collection and laboratory analysis after the field campaign, for a number of environmental parameters. Indeed, new dynamic positioning systems, lighter and cheaper sensors are available, and will be even more in the near future, yielding to an explosion of georeferenced, highly accurate data for many different purposes. Having a real-time punctual measurement of an environmental variable opens the door to new on-the-fly sampling decisions. On the other hand, this requires innovative computational solutions to make data analysis precise and fast.

In environmental survey, beside an estimate map representing the phenomenon under examination, it is crucial to know the accuracy of the estimations, allowing experts to take more informed decisions. In fact, human factors and the tools or analysis tech-

DOI: 10.2312/stag.20181306

niques applied can all introduce uncertainty in the data and, subsequently, in the representation of the reconstructed reality. Until now the concept of uncertainty has had a “passive” role, since it was only used retrospectively as a tool to measure the accuracy of the model. However, its role can become “active” by intervening in the definition of a new sampling strategy, based on *uncertainty minimization*.

We present an innovative adaptive sampling schema where the optimization is based on a measure of uncertainty. The approach does not require predefined samples, but conversely the adaptive strategy follows an iterative selection of samples in a way that minimizes the uncertainty of the estimates. Our formulation of the concept of "uncertainty" relies on making several estimates for the value at each point and computing the variance: intuitively, this measures how much such estimates are reliable. Since the analysis occurs in real time it is possible to use the information just acquired to take conscious decisions promptly.

In this paper, we provide an adaptive sampling algorithm to drive a robotic platform during an environmental survey. When sampling soil, water or air, many different types of equipment are needed. We provide a general framework that can manage multiple sensors in a modular fashion. We also evaluate the accuracy of the method by implementing a remotely operated vehicle simulator. We present our preliminary results on a bi-dimensional synthetic scenario, and draft the ongoing generalization of these encouraging outcomes to the full 3D domain for water quality monitoring in harbours. A proper geometric representation of the three dimensional survey area, which may be arbitrarily complex, beside encoding the domain constraints and optimizing the processing, allows for a proper visualization of variable distribution and related uncertainty.

The contribution of this work is to pose the basis to develop an integrated system where the adaptive sampling approach together with the advanced representation and visualization of the uncertainty will improve the efficiency and precision of environmental surveys while reducing time and costs.

2. Background and State of the Art

Geostatistics (Matheron, [Mat62], [Mat63]) was born in the early 1980s as a hybrid discipline of mining engineering, geology, mathematics, and statistics. Geostatistics provides the mathematical tools to build a complete distribution map over a domain given a discrete set of known values. Environmental sampling provides real measures of specific variables in a limited set of locations (samples). Environmental variables are characterized by a spatial relation among observations: close areas tend to have similar values whereas ones that are farther apart differ more. Geostatistics expresses this intuitive knowledge quantitatively and then uses it for prediction.

Kriging (Webster & Oliver, [WO07]) is a regression method used in geostatistics that allows a variable to be interpolated in space, minimizing the average quadratic error. The unknown value in a point is calculated with a weighted average of the known values. The weights that are given to the known measurements depend on the spatial relationship between the measured values in the neighborhood of the unknown point. To calculate the weights we use the *variogram*, a graph that relates the distance between two points and the variance value between the measurements made in these two points. The variogram shows, both qualitatively and quantitatively, the degree of spatial dependence in the data. The semivariogram is the function that interpolates the semivariance of the values $Z(x)$ observed in groups of pairs of points x at distance h while the distance h varies (directional distance).

For a given h, the semivariance is given by the following formula:

$$\gamma(h) = \frac{1}{2} var[Z(x) - Z(x+h)] = \frac{1}{2} E[(Z(x) - Z(x+h))^2]$$

where h, the vector representing a directional distance, is known as the *lag*. This spatial relation depends on the lag and not on the absolute position of the points x.

The semivariogram (the graph of the semivariance on the distance between the data) is normally interpolated with different functions in order to determine the type of spatial autocorrelation of the measured variable. The parameters to be estimated are:

1. Nugget: describes the random variability level;
2. Range: distance limit beyond which the data are no longer correlated;
3. Sill: describes the level of spatial variability, and is the maximum or asymptotic value that is reached at the Range.

Methods to estimate such parameters are described in the work by Cressie, [Cre85].

There are several distinct kind of Kriging to tackle increasingly complex problems in environmental studies (Webster & Oliver, [WO07]). We use the linear Kriging, so that the estimate at a point is simply a linear sum of the weighted average of the data in its neighbourhood. The prediction estimates are obtained with:

$$\hat{Z}(x_0) = \sum_{i=1}^{N} \lambda_i z(x_1)$$

where x_0 is target point, N is the number of known points in the neighbourhood and λ_i are the weights that must sum to 1. The estimate of λ_i relies on the variogram model and thus on the spatial variability law among points. The weights describe the influence of each neighboring point in the estimate of the target point. The calculation of λ_i is beyond the scope of this paper. See the work by Cressie [Cre85] for more details and how λ_i are calculated.

Beside traditional sampling schemes, there are some new iterative approaches that exploit the Kriging model for optimization. These methods have concentrated upon the minimization of the Kriging variance related to the sampling pattern (van Groenigen et al. [vGSS99] [vG99]; Lark, [Lar02]) or upon an approximation of the variogram uncertainty (i.e variance-covariance matrix of the fitted parameters of the variogram) (Marchant & Lark, [ML03]).

Another example of iterative approach is in the work by van Groenigen et al. [vGSZ97]. The procedure is proposed to optimize environmental risk assessment. Environmental risks are quantified by the probability of exceeding the intervention level. Maps showing these probabilities are obtained with indicator Kriging (Webster & Oliver, [WO07]) and the next sampling points are selected on the base of this maps.

An alternative way, using a Bayesian approach, to optimize an environmental sampling and to select the next point adaptively is addressed in [XC11].

However, Kriging tends to underestimates values that are larger than average and to overestimate those that are smaller. In general, we obtain a smoothed representation of reality. In the works of Goovaerts [Goo97] and Lin et al. [LCT01] Kriging is compared with stochastic simulations and in these studies simulation techniques yielded better results than Kriging. In particular, Sequential Gaussian Simulation (SGS) provides a measure of uncertainty of the estimates.

Like the above mentioned approaches, we present an iterative method, but our sampling strategy uses a measure of uncertainty of the current prediction as optimization function. In the field of geometric modeling a geometric model, named *Fuzzy B-spline*, has been defined for the explicit representation of the uncertainty related to shapes (Anile et al., [AFG+00]). In our setting, the explicit representation of uncertainty could provide an effective tool for communicating the quality of the reconstruction and for suggesting refinements during the process. Using real-time uncertainty information, either the human expert or an automatic software can drive the survey in such a way to extract much more information with less uncertainty. In this way we can achieve more reliable representations of reality with fewer samples selected *ad hoc*.

Our work starts from some previous prototypes by Pittaluga [Pit04], Sartori [Sar13] and Semino [Sem14]. The aim of this paper is to demonstrate the potential of using adaptive sampling procedures able to select new points in real-time by minimizing the uncertainty of the estimates. Furthermore, our work aims to take advantage of geometry modeling and visualization methods to provide a real-time feedback to the final user.

3. Uncertainty-driven Adaptive Sampling

Our adaptive sampling approach is an iterative method. At each iteration, our method estimates the best next point to be sampled and updates the known information with new acquired data. Our method requires a description of the area to be sampled (e.g. boundaries, constraints) and an initial set of sampled points where the variable value is known. In the following paragraphs, we assume the survey area to be represented as a regular grid with a user-defined resolution. Section **??** describes the ongoing work on the generalization to fully 3D areas bounded by arbitrarily complex boundaries.

Starting from the initial set of sampled points, each iteration of the adaptive sampling works as follow:

1. Definition of the spatial variability law describing the observed environmental variable, based on sampled points (see Section 3.1);
2. Generation of the *spatial prediction map* and related *uncertainty map* (see Section 3.2);
3. Exploitation of the *uncertainty map* to determine the next point to be sampled (see Section 3.3);
4. Sample the new point and enrich the set of sampled points with the new measure (see Section 3.3).

The iterative loop stops when a specific desired condition is satisfied. Our current implementation considers a user-defined number of iterations as a stop condition.

3.1. Definition of the spatial variability law

The goal of this phase is to describe the spatial variability of the observed environmental variable by exploiting the set of points where the actual value is known. At the beginning of the process, the system is initialized with a small set of samples (i.e. 1% of the domain size in our experiments). At each iteration, the set of known values is enriched with newly acquired samples.

At the beginning of each iteration, we preprocess the set of known values to guarantee they follow a normal distribution. This is a requirement of geostatistics methods used to define the spatial variability low. If this condition is not satisfied, we transform them through a *normal scores transformation (NST)* (Deutsch & Journel, [DJ98]), which assumes a mean value of 0 and standard error of 1 and adjusts each sample value by mapping it from its original probability to the S-shaped curve corresponding to a normal distribution (Coburn, [Cob12]; Isaaks & Srivastava [HIRS91]). An advantage of using NST is that estimated values can be transformed back to real values by applying an inverse NST.

We describe the spatial correlation among real observations through the variogram, fitting it with a mathematical function defined in terms of range, sill and nugget. Our implementation estimates the three parameters using the *ordinary least squares* method (Cressie, [Cre85]). Once the spatial variability has been estimated, we proceed with estimating the prediction over unsampled areas and calculating the uncertainty related to that prediction.

3.2. Variable prediction and uncertainty evaluation

We use the Sequential Gaussian Simulation (Webster & Oliver, [WO07]) to estimate the variable over the domain and measure the uncertainty at each point. SGS is a method for simulating a multivariate Gaussian field, where each value is simulated sequentially according to its normal conditional cumulative distribution function, which must be determined at each location to be simulated.

The input data of a SGS is the set of known values and their spatial variability low, together with the description of the survey area. A single SGS works as follows:

1. Determine the sequence in which the points in the domain will be visited for each simulation (e.g., randomly).
2. Simulate at each point p:
   - Use kriging to obtain $\hat{Z}(p)$ and $\hat{\sigma}^2_K(p)$
   - Draw a value v at random from a normal distribution: $N(\hat{Z}(p), \hat{\sigma}^2_K(p))$
   - Map point p to value v and add it to the SGS set of known values.

The output of a single SGS is a map where each point is associated to its estimated value. We run a set of SGSs (i.e. 20 in our implementation) and we finally map each point to the average of its estimations. By assigning each point its average estimated value, we generate a global *prediction map*, while a global *uncertainty*

map is built by assigning each point the variance of its estimations. These two maps provide a global overview of the variable distribution and uncertainty information. Eventually, the uncertainty map enables the adaptive selection of the next point to be sampled as the one where the uncertainty is highest.

3.3. Next point to be sampled

The final goal of our method is to provide a representation of reality as reliable as possible. Thus, the next point to be sampled must improve the reliability of the estimations. With this final goal in mind, the selection of the next point to be sampled is guided by the *uncertainty map* generated in the previous step, from which we can easily detect the points where the variance of the estimates is highest. The addition of new sampled points in regions of high uncertainty leads to a better representation of reality while reducing the estimation uncertainty. The point with highest uncertainty will be the next to be sampled. While moving from the current position X_c to the selected next point X_n, we can imagine two cases: only the extremes of the path X_c and X_n are sampled, or the sampling is continuously performed along the path (X_c, X_n), adding all points in between to the set of known points. The two situations depend on the modality in which the survey is carried out and on the sensors employed. For example, if we imagine a human operator performing soil sampling with a X-ray fluorescence spectroscopy (XRF) hand-held sensor, only the locations at X_c and X_n will be measured. Conversely, in the case of an underwater vehicle equipped with a sensor for salinity able to measure continuously, it makes no sense to discard measurements that are anyway performed by the sensor along the way, and therefore all points along (X_c, X_n) will be measured.

Although this approach actually increases the reliability of the representation of the reality, it only aims to minimize the uncertainty of the estimations, and does not take into account other possible costs coming from real applications (i.e. the cost of moving from one point to a point very far away). In theses cases, the minimization function needs to be adapted to the specific costs to be optimized. An improvement of this approach considers uncertainty areas rather than punctual uncertainty. This is because a single point may have high uncertainty, but the representation of the surrounding area may be already sufficiently reliable. Then, the next point to be sampled should be selected as the one surrounded by the most uncertain area. Thus, our implementation provides the possibility to minimize the uncertainty while trying to optimize the displacement of the mobile platform (human operator) by selecting, among the N points with higher uncertainty, the one with minimum distance to the current position. N is a parameter that can be tuned as appropriate. The selection procedure of the new sampled point is represented in the Algorithm 1 with a pseudo-code. Other implementations may consider different costs and specific weights.

Algorithm 1

input ← *Grid points in the uncertainty map*
output ← *Next sample*
N ← *user's parameter*

1: Sort points in input by uncertainty in decreasing order.
2: Calculate the distance of each point respect with current position
3: Select first N points in ranking
4: Among the N points return the point with the minimum distance to the current position.

4. Results and Discussion

We implemented a prototype of the uncertainty-driven adaptive sampling using the *R* software ([R C]) and set up an experiment to evaluate the approach.

For the experiment, we generate an input synthetic survey area by exploiting a library providing geostatistics methods, GSLIB (Deutsch & Journel [DJ98]). We set different variogram parameters (nugget, sill and range) and different sets of synthetic samples to control the shape of the statistical distribution. The survey area is represented as a bidimensional grid of values that mimics the real area to be sampled (Figure 4(a)). The variable distribution in our synthetic datasets satisfies the normality condition. We consider in particular the complex case of an underwater robotic platform equipped with sensors and implemented a simulator to replicate the uncertainty-driven adaptive sampling of the synthetic survey area. The simulator implements the kinematics law to mimic the platform motion from a start point to an end point. The experiment is set in a bi-dimensional space, but our goal is to extend the approach to the 3D case, specifically to address the path planning of a ROV for water quality monitoring in harbours. The cruise speed and acceleration of the vehicle is defined by the user. For the sake of generality, the hardware simulator is highly customizable and enables the possibility to virtually equip the platform with different sensors, each of them responsible for sampling a different variable and having its own sampling rate and communication delay. Results in this paper, however, consider a single variable at a time.

4.1. Experimental results

The input of our experiments is a synthetic survey area with resolution 100x100. From the input survey area, we select an initial set of sampled points through the adaptive procedure. The set $S = \{p_1, p_2, ..., p_n\}$ of initial samples points can be enriched by the measurements acquired by sensors along the path between each pair of consecutive points p_i and p_{i+1} in S. In our experiments, n is set to 10.

Figure 1 shows an example of spatial prediction map (on the left) and the corresponding uncertainty map (on the right) of the simulated survey area at the end of the whole iterative process (20 iterations). At each iteration, the next point to be sampled is selected as the one having the maximum uncertainty while trying to avoid too long displacements. This is done by selecting the new point as the most uncertain one among the points closest to the current position. Figure 2 shows how the variogram and its fitting change at each iteration.

4.2. Validation

Our simulated synthetic environment enables the possibility to compare results with the "real data" (i.e., the synthetic survey area),

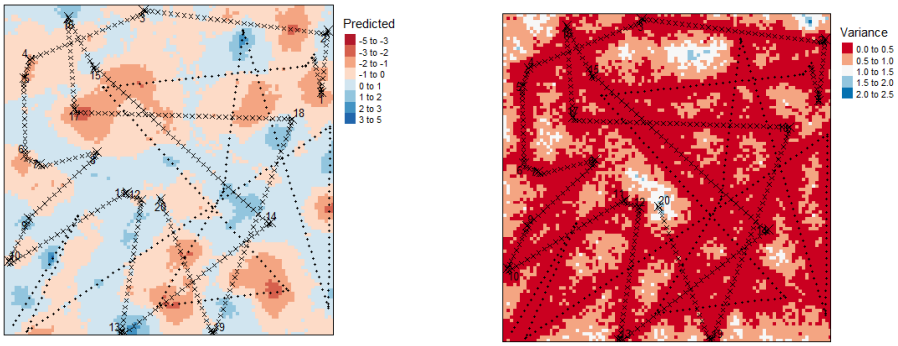

Figure 1: *Spatial prediction map (left) and uncertainty map (right).*

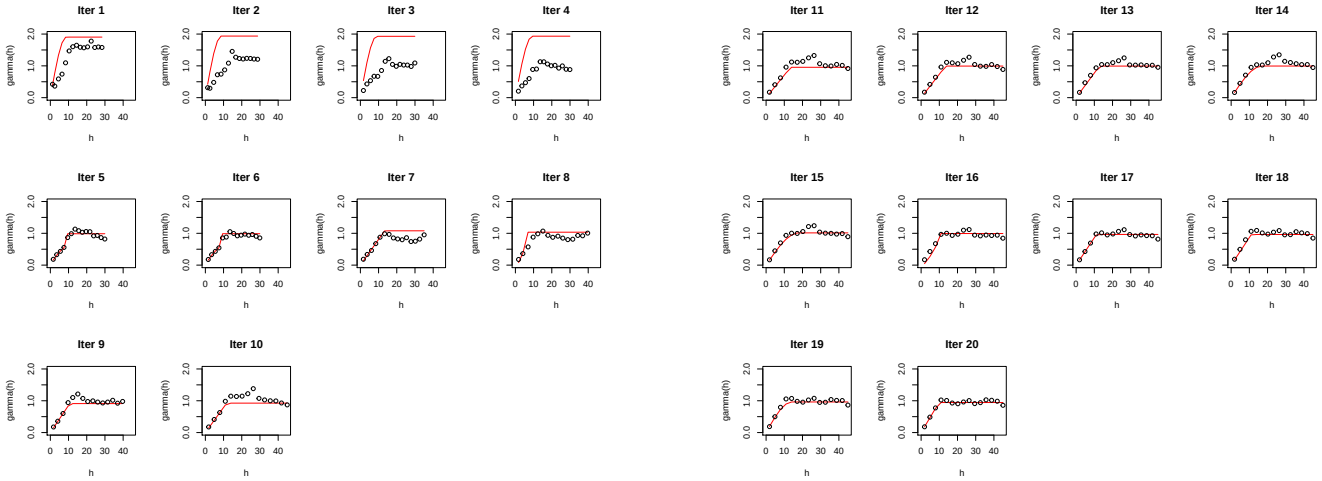

Figure 2: *Variograms and their fits (red line) for each iteration of entire sampling.*

which is impossible in the real world. We use this information as a ground truth to evaluate the reliability of our approach. Reliability is measured as Mean Square Error (MSE) between reality and estimated values:

$$MSE = \sum_{i=1}^{n} (\hat{Y}_i - Y_i)^2$$

where n is the number of cells in the grid, $\hat{Y}$ are the estimated values from SGS and Y are the real data. Our simulated field is shown in Figure 4(a).

In Figure 3 two graphs are shown. The graph on the left underlines a decreasing trend of the MSE while increasing the number of samples. However, when a sufficiently good number of sampled point is reached (i.e. thirty in our case), the MSE seems to be stable and its decrease is not relevant anymore. Similarly, the graph on the right shows the difference between MSE in two subsequent iterations. In other words, it measures the improvement provided by a new adaptively sampled point. Again, after about thirty adaptive samples this difference tends to zero. These two graphs suggest the choice of a feasible stop criterion. Indeed, adding new samples after a certain number does not add enough information compared to the costs of sampling. Nevertheless, in the real case, the real data is unknown and, thus, MSE with respect to the reality cannot be evaluated this way.

4.3. Comparison with traditional sampling

To demonstrate that adaptive sampling actually allows to get an informative result as precise as the traditional methods (sampling on regular grid) while reducing sampling efforts, we compare the prediction maps and measure their reliability with respect to reality (Figure 4(a)) using the MSE. For the sake of a fair comparison, we discard values acquired during the mobile platform displacement and keep only measures at the begin and end of route, and set the number of adaptive sampled points to a fixed amount (i.e. 100 in our experiment). Figure 4(b) shows the prediction map referred to our adaptive sampling scheme, while Figure 4(c) shown the prediction map of traditional sampling on regular grids using always SGS. By looking at the MSE values, it is evident that, for the same number of samples, adaptive sampling is more reliable than the traditional method. The regular grid sampling indeed studies

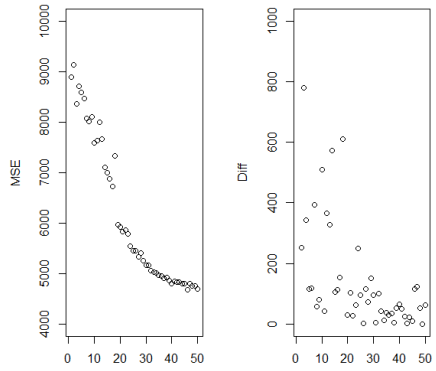

Figure 3: *Behavior of the MSE for each iteration (left) and of the differences between two successive iterations (right).*

the environmental phenomenon at a predefined resolution: the cell dimension corresponds to the minimum sampling interval. If this value is not small enough, we risk to loose important information about the behavior of the variable between the sample points, and the estimate will be rough in these zones. If the minimal sampling interval is too small, we risk to over-sample the field.

4.4. Computational complexity

To evaluate the computational complexity we studied the running time of the algorithm on fields of different resolutions. In particular, we simulated a field on 1024x1024, 768x768, 512x512, 256x256 and 128x128 grids and we estimated the environmental variable. In Table 1 we report, for each resolution, the timing of the first and last of the ten iterations, the average iteration time, the average time for the SGS procedure, which is the most demanding, and the total computation time.

Table 1: *Running time of the algorithm at different resolutions of the same field (1024x1024, 768x768, 512x512, 256x256, 128x128).*

	Running time				
	Iteration 1	Iteration 10	Mean Of iterations	Mean of SGSIM	Total (10 iterations)
1024x1024	00:02:05	00:02:09	00:02:09	00:01:49	00:21:29
768x768	00:01:07	00:01:09	00:01:09	00:00:59	00:11:29
512x512	00:00:30	00:00:28	00:00:29	00:00:24	00:04:50
256x256	00:00:07	00:00:08	00:00:07	00:00:06	00:01:11
128x128	00:00:02	00:00:02	00:00:02	00:00:01	00:00:19

Obviously, the running time increases with the resolution. Figure 5 depicts the running time with respect to the grid resolution in terms of number of cells. The plot nicely exhibits a nearly linear behaviour.

The part of the algorithm that weighs more on the running time is the calculation of the SGS with GSLIB. In the case of maximum resolution, at each iteration the algorithm must estimate (ten times, if the parameter of the number of simulations is set to ten) about one million cells and this effort has strong repercussions on the timing. In a real-world scenario experts should find a compromise between the running time and the desired resolution.

5. Conclusions and Future works

We propose a new approach to adaptively sample environmental variables. Using the uncertainty map as a criterion for optimization, the adaptive sampling provides the same level of information of traditional methods with a minor number of samples. Thanks to the uncertainty map, our method detects those points where more information is needed (i.e. the more uncertain ones) and enables the possibility to iteratively enhance precision and reliability by adding to the model salient information.

We implemented a simulator to carry out preliminary testing of the system. In our experiment, adaptive sampling showed an excellent performance for environmental survey with respect to the traditional techniques.

This result motivates further research towards the definition of new efficient and cost-effective environmental surveys. Other definitions of uncertainty could be investigate and new selection strategy of next point could be considered in a future implementation. For example, we are evaluating to consider the parameter N as a distance threshold, that set a radius of a circumference with the center in the current position. In this circumference the next uncertain point must be selected. On this new strategy we still have to verify convergence.

The most important future work addresses the shift to volumetric representations of survey areas. So far, the description of our adaptive sampling algorithm assumes the survey area to be described as a regular 2D grid. This representation, valid in other environmental sampling surveys, is used in this paper as a preliminary case study and is suitable to represents planar and rectangular survey areas. Nevertheless, in real applications the survey area may easily have arbitrarily complex boundaries and may have a volumetric nature. We are particularly interested in water quality estimation in harbours, where a ROV can move in the three dimensions, in an area typically constrained by non-convex boundaries (e.g., pier structures). Our method is general and can be theoretically applied to any survey area, as far as the domain can be represented as a 3D geometric model where the boundaries are explicitly encoded (see Figure 6 and 7)

Structured voxelizations are the direct extension of 2D regular grids and enable to represent rectangular areas with a specific resolution. Nevertheless, representing free-form areas through a regular voxelization may end up with a high resolution model made of millions of small elements, difficult to be handled by our algorithm due to the high dimensions. Tetrahedral meshes are more suitable to represent free-form areas, and they allow a multi-resolution representation of the area where the discretization resolution can be locally adapted where needed. Beside the state of the art, polyhedral meshes including cells of different form are even more flexible and will be investigated in the next steps.

Starting from these considerations, we aim to improve our tool to support free-form height field and volumetric areas and to consider

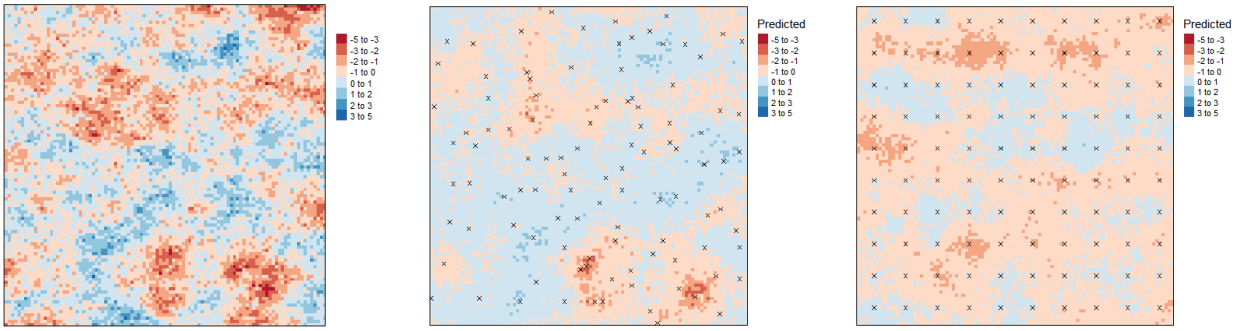

(a) (b) (c)

Figure 4: *(a) Synthetic variable distribution representing reality in our experiment, (b) Spatial prediction map with adaptive sampling (MSE = 8838.204) and (c) sampling on regular grid (MSE = 13757.02).*

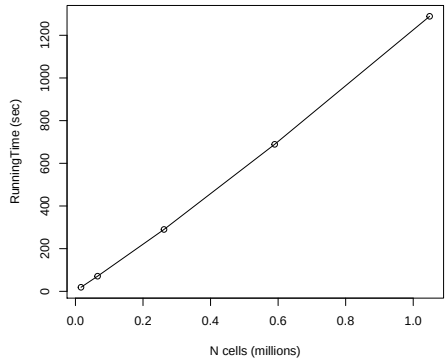

Figure 5: *Behaviour of running times (in seconds) with the increasing of the number of cells of the grid (in millions) on which algorithm estimates the environmental variable.*

the geometric and physics constraints given by the morphology of the surveyed area. Furthermore, we aim to visually represent the uncertainty information on the 3D model so that experts can supervise the adaptive sampling in real time.

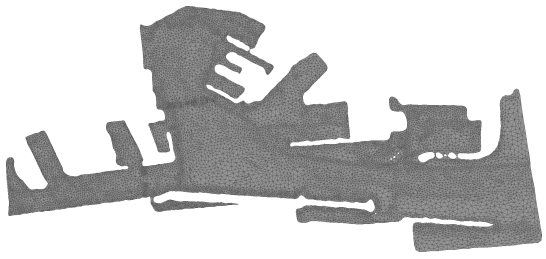

Figure 6: *An example of height field survey area with arbitrarily complex boundary constraints. The survey area is represented as a 2.5D triangle mesh.*

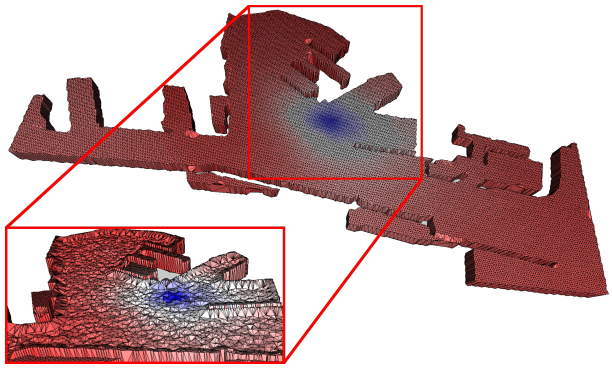

Figure 7: *An example of a volumetric survey area, represented as a tetrahedral mesh. In the bottom left frame, an internal layer is shown. The color associated to each vertex represents the value of the simulated environment variable at the vertex position. The variable satisfies the normality condition.*

6. Acknowledgement

This research is financed by the project "Monitoraggio Adattivo in Tempo reale con Automatizzazione del Campionamento - Aree Costiere Portuali - MATRAC-ACP", funded by the EU Interreg V-A Italia Francia Marittimo 2014-2020 - Asse prioritario del Programma 2 - Protezione e valorizzazione delle risorse naturali e culturali e gestione dei rischi - Obiettivo specifico della Prioritá d'Investimento 6C2-Accrescere la protezione delle acque marine nei porti.

References

[AFG+00] AM Anile, Bianca Falcidieno, Giovanni Gallo, Michela Spagnuolo, and Salvatore Spinello. Modeling undertain data with fuzzy b-splines. *Fuzzy sets and systems*, 113(3):397–410, 2000. 3

[Cob12] T Coburn. Practical geostatistics: Modeling and spatial analysis. 44:83–84, 01 2012. 3

[Cre85] Noel Cressie. Fitting variogram models by weighted least squares. *Journal of the International Association for Mathematical Geology*, 17(5):563–586, 1985. 2, 3

[DJ98] CV Deutsch and AG Journel. Gslib user's manual. *Oxford University Press, New York*, 1998. 3, 4

[Goo97] Pierre Goovaerts. Kriging vs stochastic simulation for risk analysis in soil contamination. In *geoENV IâĂŤGeostatistics for Environmental Applications*, pages 247–258. Springer, 1997. 3

[HIRS91] Edward H. Isaaks and Mohan R. Srivastava. An introduction to applied geostatistics. 33, 11 1991. 3

[Lar02] R.M Lark. Optimized spatial sampling of soil for estimation of the variogram by maximum likelihood. *Geoderma*, 105(1):49 – 80, 2002. 2

[LCT01] Yu-Pin Lin, Tsun-Kuo Chang, and Tung-Po Teng. Characterization of soil lead by comparing sequential gaussian simulation, simulated annealing simulation and kriging methods. *Environmental Geology*, 41(1-2):189–199, 2001. 3

[Mat62] Georges Matheron. *Traité de géostatistique appliquée. 1 (1962)*, volume 1. Editions Technip, 1962. 2

[Mat63] Georges Matheron. Principles of geostatistics. *Economic geology*, 58(8):1246–1266, 1963. 2

[ML03] BP Marchant and RM Lark. Adaptive schemes for geostatistical sampling and survey. In *MODSIM 2003: International Congress on Modelling and Simulation*, pages 1709–1714. Citeseer, 2003. 2

[Pit04] Simone Pittaluga. Determinazione della concentrazione di analiti potenzialmente pericolosi (phes) in domini spaziali irregolari con metodi stocastici, 2004. Master Degree Thesis. 3

[R C] R Core Team. *R: A Language and Environment for Statistical Computing*. R Foundation for Statistical Computing, Vienna, Austria. 4

[Sar13] S. Sartori. Enviromental real-time sampling: optimal sampling schema based on stochastic spatial variance., 2013. Master Degree Thesis. 3

[Sem14] F. Semino. Application of a âĂIJreal-timeâĂİ adaptive sampling schema to the caldara manziana spontaneous co2 high emission area (monti della tolfa, roma), 2014. Master Degree Thesis. 3

[vG99] Jan-Willem van Groenigen. *Constrained optimisation of spatial sampling*. Number 65. [sn], 1999. 2

[vGSS99] J.W. van Groenigen, W. Siderius, and A. Stein. Constrained optimisation of soil sampling for minimisation of the kriging variance. *Geoderma*, 87(3):239 – 259, 1999. 2

[vGSZ97] J.W. van Groenigen, A. Stein, and R. Zuurbier. Optimization of environmental sampling using interactive gis. *Soil Technology*, 10(2):83 – 97, 1997. 2

[WO07] Richard Webster and Margaret A Oliver. *Geostatistics for environmental scientists*. John Wiley & Sons, 2007. 2, 3

[XC11] Yunfei Xu and Jongeun Choi. Adaptive sampling for learning gaussian processes using mobile sensor networks. *Sensors*, 11(3):3051–3066, 2011. 3